ATMOSPHERIC ENVIRONMENT: X 16 (2022) 100192

Contents lists available at ScienceDirect

Atmospheric Environment: X

journal homepage: www.journals.elsevier.com/atmospheric-environment-x

Comparing an energy-based ship emissions model with AIS and on-board emissions testing

Robin Smit [a,b,e,*], Thuy Chu-Van [c,d], Kabir Suara [c,f], Richard J. Brown [c]

[a] Department of Environment and Science, GPO Box 2454, Brisbane, QLD, 4001, Australia
[b] University of Technology Sydney, Faculty of Engineering and Information Technology, Sydney, Australia
[c] Biofuel Engine Research Facility (BERF), Queensland University of Technology (QUT), QLD, 4000, Australia
[d] Vietnam Maritime University (VMU), Haiphong, 180000, Viet Nam
[e] Transport Energy/Emission Research, Brisbane, QLD, 4068, Australia
[f] Water and Environment Group, BMT Commercial Australia, Osborne Park, WA, 6017, Australia

ARTICLE INFO

Keywords:
Shipping
OGV
Emissions
On-board emission testing

ABSTRACT

On-board emission testing data for two ocean-going vessels is used to assess the performance of a new Australian ship emissions model, and to also assess the impact of local currents on emission predictions. Prediction performance is only marginally affected by AIS post-processing method and inclusion of local current information. Model performance was assessed for three different aspects, fuel-based emission factors (g/g CO_2), engine work-based emission factors (g/kWh) and distance-based emission factors (g/km). Analysis of fuel-based and engine-work based emission factors suggest good performance and small to reasonable mean prediction errors for CO_2 (±10%), PM_{10} (±15%) and SO_2 (±20%). For NO_x and CO, on-board emissions testing suggest that model emission factors are biased high and low with mean prediction errors +60–70% and −60%, respectively. The results for distance-based emission factors were not considered to be meaningful due to spatial and temporal inaccuracies in linking on-board testing with the AIS data that could not be resolved. Given the importance of AIS data as input to fuel and emissions modelling, it is recommended that the spatial and temporal accuracy of AIS data is investigated and confirmed in future studies. Moreover, the differences found in this study between model predictions and on-board measurements highlight a few limitations in application of generic fleet-based models.

1. Introduction

Shipping is a significant source of air pollution and greenhouse gas emissions. Ships use large diesel engines that run on heavy bunker fuels, generally without emission controls. Overseas studies have consistently found that ships have significant effects on local air quality in and around port areas (e.g. EEA, 2013). Corbett et al. (2007) estimated that 3 to 8 per cent of global $PM_{2.5}$ related mortalities are attributable to marine shipping. Liu et al. (2016) reported that container ships and bulk carriers are the main contributors in East Asia for all pollutants, except methane, leading to an estimated 14,500–37500 premature deaths per year.

In previous research (DES, 2019), an Australian ship (exhaust) emission model was developed that uses detailed data on local ship movement and ship characteristics. The model first estimates fuel use and subsequently uses fuel-based emission factors (g/kg fuel) to estimate emissions. The model is based on extensive literature review and model parameters were calibrated at fleet level using an energy balance approach. In this study, model performance is evaluated using independent on-board emissions testing data for two ocean-going vessels. In addition, new avenues for model improvement are explored, which includes inclusion of the impacts of sea currents.

As will be discussed in Section 2.2, the Australian ship emission model has several communalities compared with other methods used internationally. In terms of ship classification, for instance, it explicitly considers engine speed category, fuel type and emission control standard (Grigoriadis et al., 2021), but also ship type, engine type and mode of operation (EMEP/EEA, 2016; EMEP/EEA, 2021; CARB, 2022). In other aspects the approach can be slightly different. For instance, the Australian model directly estimates fuel use (kg/min) as a function of ship operating conditions (engine load, operating mode) and then estimates greenhouse gas and air pollutant emissions using fuel-based

* Corresponding author. Department of Environment and Science, GPO Box 2454, Brisbane, QLD, 4001, Australia.
E-mail address: robin.smit@transport-e-research.com (R. Smit).

https://doi.org/10.1016/j.aeaoa.2022.100192
Received 4 August 2022; Received in revised form 23 October 2022; Accepted 30 October 2022
Available online 1 November 2022

emission factors (g/kg fuel). These emission factors are constant above 20% engine load (MCR) but increase below 20% MCR for pollutants such as NO_x, PM, CO and HCs.

This low load emission factor adjustment is also used in US emission inventories (CARB, 2022; US EPA, 2022). In comparison, Grigoriadis et al. (2021) used separate emission algorithms for each air pollutant, expressing emissions as mass of pollutant per unit of energy produced by the engine. In this model, the base emission factors (g/kWh) are constant but vary with engine, fuel and emission control and are modified according to operational engine load. Ship emission inventory methods used in the USA (CARB, 2022; US EPA, 2022) also use emission factors expressed as g/kWh, where operational engine load is commonly estimated by combining (default or propellor/admiralty law derived) load factors with vessel-specific rated engine power. The European Emission Inventory Guidebook (EMEP/EEA, 2016; EMEP/EEA, 2021) offers both options (fuel-based or load-based emission factors) for its most detailed Tier 3 emission inventory method.

2. Method

2.1. On-board emissions testing

The on-board emission testing was carried out in October and November 2015 on two large cargo ships under different operating ship conditions at berth and during manoeuvring and cruising. The first on-board emission measurements were conducted on a general cargo ship during her voyage from Port of Brisbane to Port of Gladstone, while the second one was performed on a bulk carrier during her passage from Gladstone to Newcastle. Table 1 presents ship characteristics for two vessels with on-board emissions testing. More detailed information about the two measured vessels in this campaign can be seen in the previous studies (Chu-Van et al., 2018, 2019).

Emission sampling points were located on a deck in the machinery room where exhaust gas from the main engines was sampled and measured continuously. The sampling position for the general cargo ship was located before the economiser (approximately 10 m of exhaust pipe from the exhaust manifold of the main engine). For the bulk carrier the sampling position was about 0.5 m after the turbocharger of the main engine. At each exhaust sampling position, two sampling holes were cut in the exhaust channel for both particle and gaseous phase measurements using the same configuration for the two vessels.

The raw hot exhaust gas was sampled directly to the DMS 500 (Cambustion, Cambridge, UK) dilution systems (2-stage dilution systems) from the first sampling hole. Raw exhaust was first diluted with hot air at a temperature of 150 °C and at a fixed dilution ratio (DR) of 5. The diluted sample was then transferred to the second dilution stage via a heated sampling line to prevent condensation of water and volatile organic compounds (VOCs). The secondary dilution stage was a high ratio rotating disc diluter with a DR range of 20–500. A DMS 500 was used to measure particle number size distributions in the size range of 5 nm–1.0 μm with a sample frequency of 1 Hz. The second sampling hole was used for measurements by a Testo 350 Portable Emission Analyser, and by a DustTrakTM Aerosol Monitor 8530 (TSI Incorporated, Minnesota, USA) and Sable CO_2 Monitor through an Ejector Diluter (Dekati, Kangasala, Finland). The concentration of gases, including sulphur dioxide (SO_2), nitrogen oxides (NO_x), carbon monoxide (CO), oxygen (O_2) and CO_2 in the raw exhaust were measured by a Testo 350 Portable Emission Analyser, while a DustTrakTM Aerosol Monitor 8530 was used to measure mass concentrations of PM_{10}, $PM_{2.5}$ and $PM_{1.0}$. More specifications of measurement devices used in the present study can be seen in our previous studies (Chu-Van et al., 2018, 2019).

2.2. Ship emission model

An energy-based ship (exhaust) emissions model was used to estimate fuel use and emissions at a high resolution for a broad range of air pollutants for ships operating in fifteen strategic port areas in Queensland, Australia, over a full year (2015). Emission simulations were conducted at a minute-by-minute resolution for individual ships operating in the port areas, after which emissions were aggregated to 1 × 1 km grid cells and allocated to each hour of the year. A full description and parameterisation of the fuel and emission prediction algorithms for the various ship types can be found in DES (2019). Table 2 presents the fuels use algorithms for the two ships investigated in this study.

Building on earlier research (Grigoriadis et al., 2021; Herzfeld et al., 2016), the fuel algorithms first predict typical fuel consumption rates for different ship classes in four modes of operation, 'transit', 'manoeuvring', 'berth' and 'anchor'. Fuel rates for moving ships in transit are simulated as a function of ship class, ship size, service speed and actual vessel speed. The predicted fuel rates represent fleet average values, but real-world variation will occur. For instance, weather and sea conditions can significantly alter the power demand in the main engine propulsion system.

Fuel rates for stationary ships are simulated as function of ship class and ship size. Once in port, power requirements for ships are usually reduced, but can still vary depending on the type of ship activity, such as hoteling, cargo refrigeration and loading operations (cargo pumps, cranes). Auxiliary engines are usually used for electric power production, while the main engines are shut down, and the boiler generates steam. The main engine is not used when ships are at berth or at anchorage, except for diesel-electric ships, where main engines may be used to generate auxiliary power.

The main ocean-going vessel (OGV) types considered in the model are: 'bulk carrier', 'container', 'cruise ship', 'general cargo', 'reefer', 'roro' (roll-on-roll-off), 'tanker (oil)', 'tanker (other)', 'vehicle carrier' and 'other'. Ship engine type is broadly defined as: 1) main engine (ME), auxiliary engine (AE) and boiler (BL), 2) slow speed (SS), medium speed (MS) and high speed (HS) diesel engines, or gas/steam turbines (GAS/STM), and 3) International Convention for the Prevention of Pollution from Ships (MARPOL) Annex VI NO_x emission certification limits, which relate to year of vessel construction, i.e. 'pre-control' (<2000), 'Tier I' (2000–2010) and 'Tier II' (2011+). Marine fuel oils are classified as follows (intermediate) residual fuel oil (RO), marine distillates (MD) and ultra-low sulphur diesel (ULSD). The fuel use and fuel-based emission factor values are similarly defined as a function of engine system, fuel type and MARPOL Annex VI emission certification limit (NO_x only), as well as operating conditions.

A ship energy-balance approach was deployed to calibrate (and expand) model parameters of the empirical functions (Table 2) to properly reflect the OGV fleet operating in Queensland waters. A ship information database was purchased from IHS Markit. These data provide detailed information for each ship that is operating in near the Queensland coast (<50 km). First, plausible ranges in ship energy use were defined. Ships travelling at service speed[1] typically use 80–90% of Maximum Continuous Rating (MCR). This is the first verification point in the energy balance. Second, plausible ranges of auxiliary engine power were determined through analysis of the IHS database and literature review. The ratios of installed auxiliary engine power to MCR were computed for all ships and plausible ranges were defined as the 10 and 90-percentile values for each ship class. Subsequently these minimum and maximum ratio values were multiplied with reported ranges of auxiliary load factors for different modes of operation.

Subsequently, a typical ship operational cycle (speed-time profile, 75 h), including all four modes of operation (cruising, manoeuvring, berth, anchor), was developed and used to predict minute-by-minute energy use for all individual ships operating near Queensland in 2015 (5510 vessels in total). Estimated fuel use (kg/min) was then converted to energy use (kW) using information on the fuel type, lower heating

[1] Service speed is defined as the speed that the ship is capable of maintaining at sea in normal weather conditions, and at normal service draught.

Table 1
Ship characteristics for two vessels with on-board emissions testing.

ID	Type	GT	Length (m)	Service Speed (knots)	Year of Manufacture	Engine Type	Propulsion	MCR (kW)	Auxiliary (kW)
Vessel 1	Bulk Carrier	27,198	188	15	2002	SSD	Oil DD	6880	1380
Vessel 2	General Cargo	31,028	185	16	1981	SSD	Oil DD	12,080	3000

Table 2
Fleet-average fuel consumption prediction algorithms [a].

Description	Vessel 1 CSL Melbourne Bulk Carrier	Vessel 2 CSL Thevenard General cargo
Main engine fuel consumption for machinery/fuel type i (kg)	$0.27S^{0.52}\ \Delta d\ p_i\ (\nu/\nu_{ss})^3$	$0.14S^{0.60}\ \Delta d\ p_i\ (\nu/\nu_{ss})^3$
Auxiliary boiler fuel consumption (kg)	$\varphi_b 0.006 S\Delta t\ /(\tau\ \eta\ )$	$\varphi_b 0.011 S\Delta t\ /(\tau\ \eta\ )$
Auxiliary engine fuel consumption for machinery/fuel type i (kg) - Transit	$0.013\ S^{0.52}\ \Delta d\ p_i$	$0.007\ S^{0.60}\ \Delta d\ p_i$
Auxiliary engine fuel consumption for machinery/fuel type i (kg) – Non-Transit	$(\ \varphi_a \psi\ 0.004\ S\Delta t - F_{boiler})\ p_x$ $\psi\ =\ 3.3\ (\tau\ \eta\ 0.004\ S\ \Delta t)^{-0.35}$	$(\ \varphi_a\ 0.007\ S\Delta t - F_{boiler})\ p_x$

S = vessel size or volume, expressed as (unit-less) gross tonnage (GT); Δd = total distance traversed by the ship (km); p_i = proportion of total fuel used by machinery/fuel type x (−); ν = actual (average) vessel speed (km/h); ν_{ss} = vessel service speed (km/h); φ_a = auxiliary engine manoeuvring correction factor (−); φ_b = auxiliary boiler manoeuvring correction factor (−); ψ = calibration function (−); F_{boiler} = auxiliary boiler fuel consumption (kg); Δt = time resolution (h); η = boiler thermal efficiency (−); τ = fuel specific lower heating value (MJ/kg).

[a] A full description and parameterisation of the fuel and emission prediction algorithms for the various ship types can be found in DES (2019), which can be accessed via https://nla.gov.au/nla.obj-1371565938/view.

value (LHV, MJ/kg fuel) and engine and fuel type dependent thermal efficiency. A robust linear regression analysis was applied to minimise prediction errors at fleet level and adjust the fuel use model parameters for the different ship types.

The model (DES, 2019) incorporates fuel-based emission factors (g of pollutant per kg of fuel burned) for air pollutants and greenhouse gases based on a review of published research reports and scientific papers (CO_2, NO_x, SO_2, PM_{10}, $PM_{2.5}$, VOCs, CH_4, N_2O, Pb, As, Ni, V, Mn, Cd, PAHs (sum), benzo(a)pyrene, 1,3-butadiene, benzene, formaldehyde, toluene, xylenes and ethylbenzene). The emission factor values are a function of engine system (ME, AE, BL), engine type (SS, MS, HS, GAS, STEAM), fuel type (RO, MD, ULSD) and MARPOL Annex VI emission certification limit (NO_x only). These emission factors are combined with estimates of fuel consumption for each minute of individual ship activity. This is done for all individual ships that operate in the study area in a selected base year and emissions are aggregated to give total emission loads. Total emission loads are aggregated at grid cell level and calculated for each hour of the year.

2.3. Ship movement data

In addition to ship parameters such as ship type and size (gross tonnage), ship emissions are critically dependent on vessel speed in a non-linear fashion. Input data regarding location and speed is therefore required at a high spatial and temporal resolution.

The on-board emission testing program did not collect data on geographic location or vessel speed and course. On-board emissions testing of on-road vehicles (PEMS) typically collect time-resolved geospatial data (e.g. location, road gradient) through access to the onboard diagnostics (OBD) system or the use of GPS sensors (Smit et al., 2022). In contrast, on-board ship emission measurements generally do not include a GPS (Khan et al., 2013). A recent paper (Grigoriadis et al., 2021) reviewed available datasets for development of ship emission factors, but the use of GPS as part of the measurement procedure was not mentioned. Another recent paper (Yang et al., 2022) did use GPS equipment, but this is one of the first papers to do so.

Therefore, ship movement information was sourced from Automatic Identification System (AIS) data. AIS is a Very High Frequency (VHF) radio broadcasting system, which enables AIS equipped vessels and shore-based ground stations to send and receive identifying information. This is known as terrestrial AIS data. In Australia, the Australian Maritime Safety Authority (AMSA) collects comprehensive AIS data. Specially equipped satellites can also record the same AIS data. AIS is a mandatory collision avoidance system on ships larger than 300 gross tonnes. Each ship transmits a signal giving details regarding the ship's identity, type, position, course over ground (COG), (spot) speed over ground (SOG) and other safety-related information at frequent intervals. Unique Mobile Maritime Service Identity (MMSI) numbers are sent in the AIS messages.

Previous research (Emmens et al., 2021) has shown that AIS data can be unrealiable and suffer from various issues such as errors (noise, human mistakes) or lack of signal (equipment failure) in static, dynamic and voyage related information such as position and SOG. In this study, a 1-min resolution is used for fuel use and emission predictions. The first step in emission prediction is the application of an AIS verification and correction protocol to improve data quality and plug data gaps. As is evident from the gaps in Fig. 1, the AIS data regularly suffers from data loss (non-connected points and lines).

To address this issue, locational data and AIS speed data were imputed with two different approaches to obtain high resolution location and speed data. Latitude-longitude (WGS84) coordinates provided by AIS were converted to UTM (zone 56 S). For gaps less than or equal to 2 h duration, UTM coordinates were linearly interpolated in space (time-steps of equal distance) using the last and first available UTM coordinates at either end of the gap. Interpolations ($\leq$2 h) were applied to a significant portion of the AIS data (about 45–55%) and generally applied to brief AIS gaps of 1–3 min. For data gaps larger than 2 h, a similar spatial interpolation is applied using a 'continuation of last recorded speed' approach. First the anticipated total distance travelled with continued last available speed is computed and compared with the actual distance between the coordinates at either end of the data gap. If the difference between these two computed distances is less than ±25%, then a linear spatial interpolation is considered reasonable.[2] Interpolations (>2 h) were applied to a small portion of the AIS data (a few percent) and concerned a single AIS gap of 4.3 h for vessel 1 and 2.4 h for vessel 2, both at cruise speed.

The spatial interpolation procedure resulted in a complete minute-by-minute time-series of geographical locations for the entire journey, after which (travel) speed and distance travelled were computed. Travel speed was computed using distance travelled between two subsequent UTM coordinates (m) and a fixed time difference (60 s). A five-pass

[2] A special situation occurs when a vessel remains in the same 1 × 1 km grid cell for a long time. Linear spatial interpolation is applied when the first and last recorded speeds at either end of the gap are less than 2.5 km/h. The inclusion of these large data gaps is important because it ensures that time periods with berth/anchorage are captured in the emissions estimation. This situation did not occur for the two vessels considered in this study.

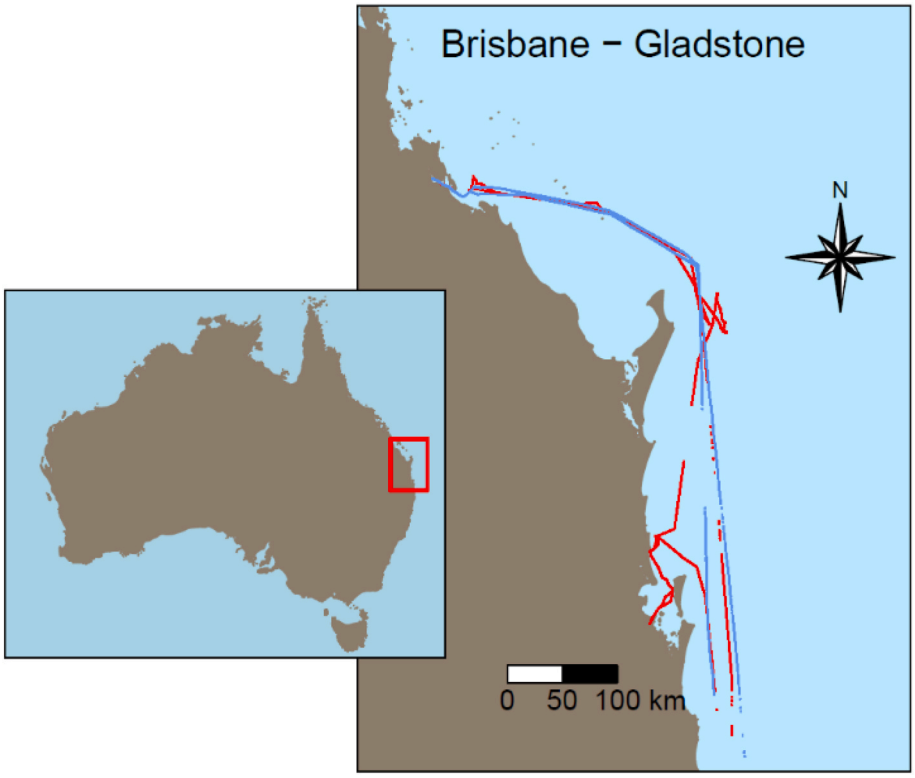

Fig. 1. AIS locational data shown as blue dot points (Vessel 1) and red dot points (Vessel 2) for two ships with on-board emission measurements. (For interpretation of the references to colour in this figure legend, the reader is referred to the Web version of this article.)

T4253H filter (Velleman, 1980) was then applied to remove noise and unrealistic variations in travel speed. Ship travel speeds less than 0.5 km/h are set to zero. A second approach was to use reported spot speeds in the AIS data (SOG, 'speed over ground'), and to use both linear and a cubic spline imputation to estimate speed values for missing SOG data. The cubic spline speed estimates were capped at the vessel service speed to prevent unrealistic speed estimates.

The result is a complete time-series for each ship journey in 1-min time steps of date-time, location (WGS84 and UTM), vessel speed (different methods) and associated vessel course over ground. This is shown in Fig. 2. There are four vessel speed and course definitions: AIS speed/course over ground (unmodified, with missing data gaps), AIS speed/course over ground (linear imputation), AIS speed/course over ground (cubic spline imputation) and location derived (UTM) speed/course over ground (T4253H filter).

2.4. *Vessel speeds corrected for current*

Engine power is dependent on speed on water, not speed over ground provided by AIS. Speed on water was estimated in this study to examine the impact on emission predictions. Vessel speeds were corrected for strength and course of local sea currents (drift). Water vectors were derived from 4 km resolution eReef model output (Herzfeld et al., 2016; eReef, 2021). Herzfeld et al. (2016) provides a detailed model description, including model calibration and validation. Briefly, eReef is a near real time regional hydrodynamic and biogeochemical model of the Great Barrier Reef developed using Sparse Hydrodynamic Ocean Code (SHOC). The model provides gridded information about spatio-temporal variation in the flow, driver (wind), and physicochemical properties (temperature, salinity, currents, density) covering the Great Barrier Reef. The three-dimensional model is based on finite difference solution

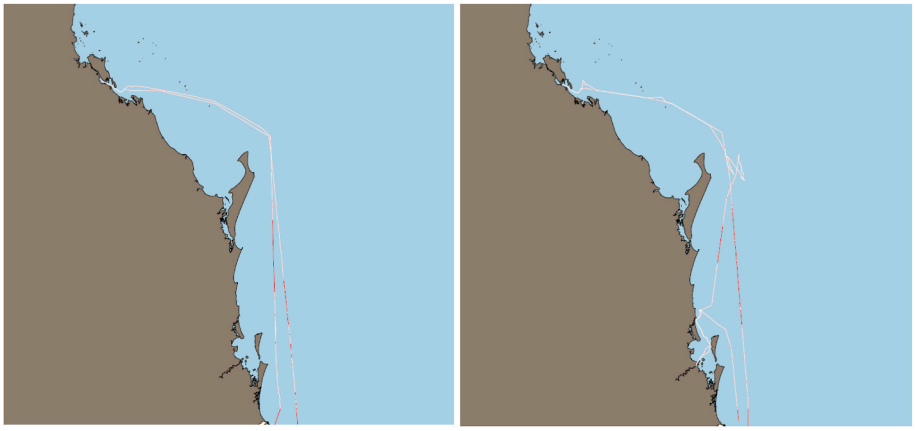

Fig. 2. Processed AIS locational data Vessel 1 (left) Vessel 2 (right), white line shows original AIS data, red line shows spatially imputed data. (For interpretation of the references to colour in this figure legend, the reader is referred to the Web version of this article.)

of primitive equations with hydrostatic and Boussinesq approximations. The hydrodynamic model uses the Australian Bureau of Meteorology's numerical weather prediction models (ACCESS-R) to provide surface forces such as the wind imposed on the model. The model has been validated with tide gauges (sea surface height), moorings (e.g. velocity), and ocean gliders (e.g. temperature and salinity) and has been used in several regional hydrodynamic studies (Baird et al., 2020; Skerratt et al., 2019; Ghosh et al., 2022). The hourly model outputs are available on 4 km grid horizontal resolution and fixed vertical z-coordinate with varying resolution (eReef, 2021).

The depth-averaged velocity covering the top 12.5 m below the mean sea level, i.e., the closest elevation to the draft of the vessels, was selected to represent the mean surface flow. A linear interpolation scheme was employed in horizontal space and time to obtain the water velocities along vessel positions (Suara et al., 2020). Vessel positions close to land and outside the spatio-temporal coverage of the eReef model were assumed to have constant and uniform water velocities, corresponding to last valid values along the vessel course. Vessel movement outside the eReef model area correspond to about a 20 km distance and 70 min.

Vessel position (UTM) was retrieved for each minute and each ship, as well as data on local currents at that location. These data were presented as displacement vectors in a Cartesian coordinate system (Easting, Northing) using information on speed (magnitude) and course over ground (angle). Easting (E) and Northing (N) vector components (orthogonal projections of speed) were computed for each minute for both vessel and local current. Speed on water was determined for each minute as the square root of the sum of the squared differences between vessel and local current (E, N) vector components.

2.5. Fuel use and emission simulation

To explore the impacts of different AIS post-processing methods, including consideration of local currents, the fuel use and emission algorithms were combined with the different time-series of vessel speed:

- **UTM**: Location derived travel speed/course over ground (T4253H filter)
- **SCL**: AIS speed/course over ground (linear imputation)
- **SCS**: AIS speed/course over ground (cubic spline imputation)
- **UTM Current**: Current corrected location derived travel speed/course over water
- **SCL Current**: Current corrected AIS speed/course over water (linear imputation)

Each time-series of vessel speed created different estimates of fuel use and emissions. Engine power (kW) was also estimated through multiplication of predicted fuel consumption (kg/s) with the lower heating value (40.5 MJ/kg), thermal engine efficiency (46%) and a unit conversion factor (1000).

2.6. Performance assessment

Various goodness-of-fit statistics can be used to assess model performance. In this study model performance is assessed with the linear Pearson correlation coefficient (r), the coefficient of determination (R^2), the mean absolute error (MAE), the mean prediction error (MPE) and the normalised root mean squared error (NRMSE).

The following rationale was considered to ensure an appropriate assessment. The aim of the paper is to compare model predictions with observations. To make sure the comparison is 'fair' and useful, the scope of the evaluation is guided by the intended application of the model for which it is designed. The emission model is not designed to make accurate predictions for individual vessels at a high time resolution (1-min time steps). Rather the model aims to provide accurate emission estimates for all OGVs (fleet level) operating in a specific study area over for instance a year. In terms of model application, the smallest spatial area of interest is typically a 1 × 1 km grid cell.

A raster file with total emission predictions at this spatial resolution can serve as input for air quality modelling and facilitates presentation of emission predictions results on maps. The minute-by-minute observed and predicted emissions data were therefore aggregated to represent vessel movement for approximately 1 km, denoted here as segments. For each of these 4050 trip segments, start and end time, total distance (km), total travel time (min), average speed (knots) and observed and predicted emission factors, expressed as (k)g/km, were computed. Segment distance varied between 800 and 1200 m and segment duration varied between 2 and 18 min. Average vessel speed varied between 2 and 14 knots. The minute-by-minute emission values were also aggregated over the three measurement time periods for each vessel to examine model performance over a longer distance and period. Distance varied between 17 and 84 km and segment duration varied between 64 and 366 min. Finally, we examined how the model performs at 'fleet level'. Given the small sample size, fleet level is narrowly defined as the average result for the two vessels combined.

Model performance is assessed in three ways:

1. Normalised for fuel use using CO_2 emissions as a proxy.
2. Normalised for engine power.
3. Normalised for travel distance as estimated with processed AIS vessel speeds.

Model performance is predicted for three different aspects, fuel-based emission factors (Method 1, g/g CO_2), work-based emission factors (Method 2, g/kWh) and distance-based emission factors (Method 3, g/km).

Method 1: This method quantifies the prediction errors in fuel-based emission factors using CO_2 as a proxy for fuel consumption. Both observed and predicted emission factors (g/min) were normalised for CO_2 (g/min) and expressed as an emission ratio. The normalised predicted and observed emission ratios were then averaged for each MCR power bin (see below) and compared.

Method 2: This method quantifies the combined prediction errors for fuel consumption and fuel-based emission factors. Both observed and predicted emission factors (g/min) were normalised for main engine power and expressed as % MCR. The normalised emissions data were then allocated to 1–100% MCR bins (5% steps) to ensure similar operating conditions, after which the predicted and observed emission factors were averaged for each bin and compared.

Method 3: This method quantifies the prediction errors for the entire emission prediction process, namely AIS processing, prediction of fuel consumption and applying fuel-based emission factors.

3. Results

3.1. The impact of AIS post-processing method on predicted vessel speed and power

The six different AIS post-processing methods (Section 2.5) can have a significant impact on the estimated vessel speeds, as is shown in Fig. 3. The grey polygon areas show the range (minimum – maximum) in estimated vessel speeds for all methods combined in cumulative time steps (minute) for the three measurement periods for each vessel.

The mean absolute difference between the maximum and minimum predicted speed for each minute is 0.3 knots for both Vessel 1 and Vessel 2. The maximum absolute differences are 1.2 knots (Vessel 1) and 1.8 knots (Vessel 2). The corresponding relative (maximum) differences are, on average, 3% (Vessel 1) and 4% (Vessel 2) and the maximum values are 18% (Vessel 1) and 30% (Vessel 2). Regarding the impact of local currents on vessel speeds, this is negligible for vessel 1 with an impact of less than 0.06% or 0.01 knots (n = 70). For vessel 2 (n = 493), the impacts are more significant varying from a speed reduction of

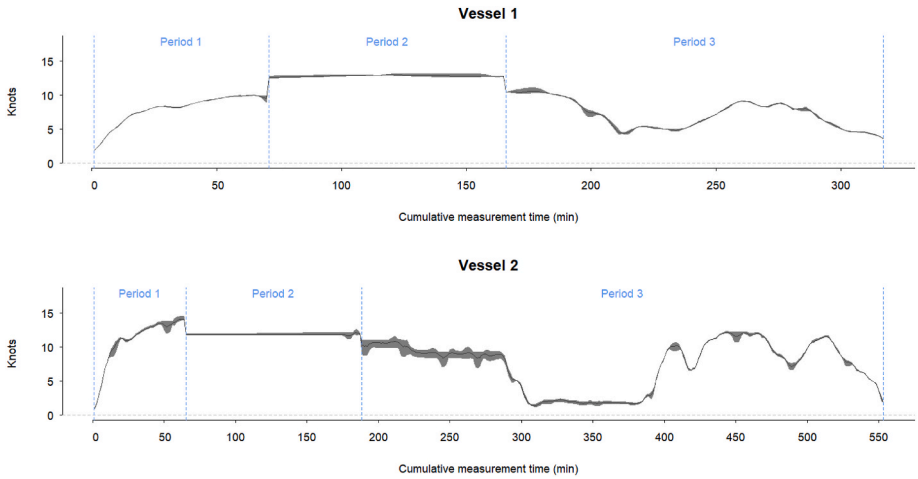

Fig. 3. The range of estimated vessel speeds using different AIS post-processing methods in cumulative minute time steps, vertical dotted blue lines demark the three different measurement periods for each ship. (For interpretation of the references to colour in this figure legend, the reader is referred to the Web version of this article.)

approximately −30% (1.2 knots) to a speed increase of approximately +15% (0.5 knots).

Given the non-linear relationship between vessel speed and main engine power, small variations in vessel speed can have a more pronounced impact on main engine power and hence fuel consumption and emissions. This is shown in Fig. 4.

The mean absolute difference between the maximum and minimum predicted main engine power for each minute is 229 kW for both vessels. The maximum absolute differences are 863 kW (Vessel 1) and 2656 kW (Vessel 2). The corresponding relative differences, expressed as a percentage of rated engine power (MCR) are, on average, 3% (Vessel 1) and 2% (Vessel 2) and the maximum values are 13% (Vessel 1) and 22% (Vessel 2). Regarding the impact of local currents on estimated main engine power, the relative impact is small for vessel 1 with less than 0.002% of MCR or less than 0.2 kW (n = 70). For vessel 2 (n = 493), the impacts are significant varying within approximately ±10% of MCR (±1200 kW).

Fig. 4 also shows that the general direction of predicted and measured power roughly aligns, but that the differences between measured and (mean) predicted power can be large. The level of agreement varies significantly from reasonable (vessel 1, period 2 and vessel 2, period 1) to poor (vessel 1, period 1 and vessel 2, period 2). The mean absolute difference between measurement and prediction is 25% of MCR for vessel 1 and 22% for vessel 2. However, the differences can be as large as 62% for vessel 1 and 56% for vessel 2. Since predicted main engine power is a critical variable in the emission algorithms, any discrepancy between measured and predicted power is an input error that will propagate through the emission calculation.

3.2. *The impact of AIS speed post-processing method on predicted emissions*

Seventy-five goodness-of-fit plots were created for three vessels (vessel 1, 2 and fleet), five pollutants, five AIS postprocessing methods and two levels of aggregation for Method 3. They are presented in the Supplementary Information (SM1). Table 3 shows model performance at fleet level. A complex picture emerges. It is not possible, based on the available evidence, to declare a superior AIS speed post-processing method because the goodness-of-fit depends on the pollutant and the performance statistic. However, the differences in performance of the three post-processing methods are marginal, which implies that the choice for a particular method will not have a significant impact in terms of model performance. Therefore, the UTM method will be used in the analysis presented in the remainder of this paper.

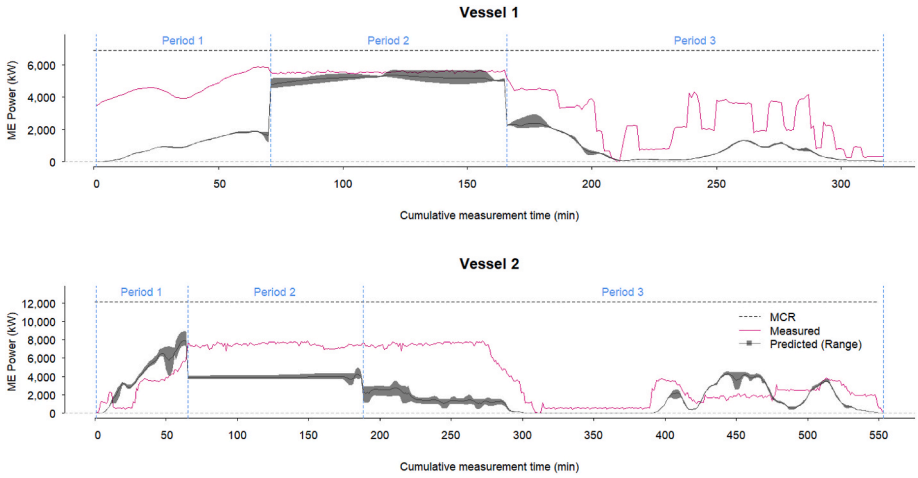

Fig. 4. Measured on-board power and the range of estimated main engine power using different AIS post-processing methods in cumulative minute time steps, vertical dotted blue lines demark the three different measurement periods for each ship. (For interpretation of the references to colour in this figure legend, the reader is referred to the Web version of this article.)

Table 3
Performance statistics for 1 km vessel movements at fleet level.

Pollutant	Speed Processing Method	r	R^2	MAE (kg/km[a])	MPE	NRMSE
CO_2	UTM	−0.08	0.01	84.77	−40%	39%
	SCL	−0.08	0.01	87.98	−40%	43%
	SCS	−0.07	0.01	86.44	−39%	43%
NO_x	UTM	−0.13	0.02	1.19	−6%	33%
	SCL	−0.17	0.03	1.17	−4%	32%
	SCS	−0.15	0.02	1.17	−4%	32%
SO_2	UTM	−0.26	0.07	0.89	−18%	35%
	SCL	−0.36	0.13	0.91	−15%	35%
	SCS	−0.33	0.11	0.90	−15%	35%
PM_{10}	UTM	−0.29	0.09	0.13	−30%	17%
	SCL	−0.31	0.09	0.14	−30%	17%
	SCS	−0.30	0.09	0.13	−29%	17%
CO	UTM	−0.46	0.21	0.24	−65%	18%
	SCL	−0.47	0.22	0.24	−65%	18%
	SCS	−0.45	0.21	0.24	−65%	18%

[a] For PM_{10} the unit is g/km.

3.3. Assessment of model performance (Method 1)

In this section emission model performance is assessed for fuel-based emission factors using CO_2 emission as a proxy for fuel consumption. As a first step observed and predicted emission factors (g/min) for each segment (approximately 1 km of vessel movement) were normalised for CO_2 (g/min) and expressed as a pollutant-to-CO_2 emission ratio. The normalised predicted and observed emissions data were then averaged for each power bin and compared. Fig. 5 (next page) compares the mean observed and predicted emission ratios for all pollutants and twenty-one engine power bins, where power is expressed as % MCR (0–100% in 5% increments). The 95% confidence intervals are included for measured emission factors, as well as the range of predictions in each power bin, whenever data are available. Table 4 presents an overview of model performance statistics.

The emission model uses fuel-based emission factors for main engines that are constant across a range of power settings, except for low power conditions <20% MCR (for instance during manoeuvring) where emission factors for NO_x, PM_{10} and CO increase. This is visible in Fig. 5

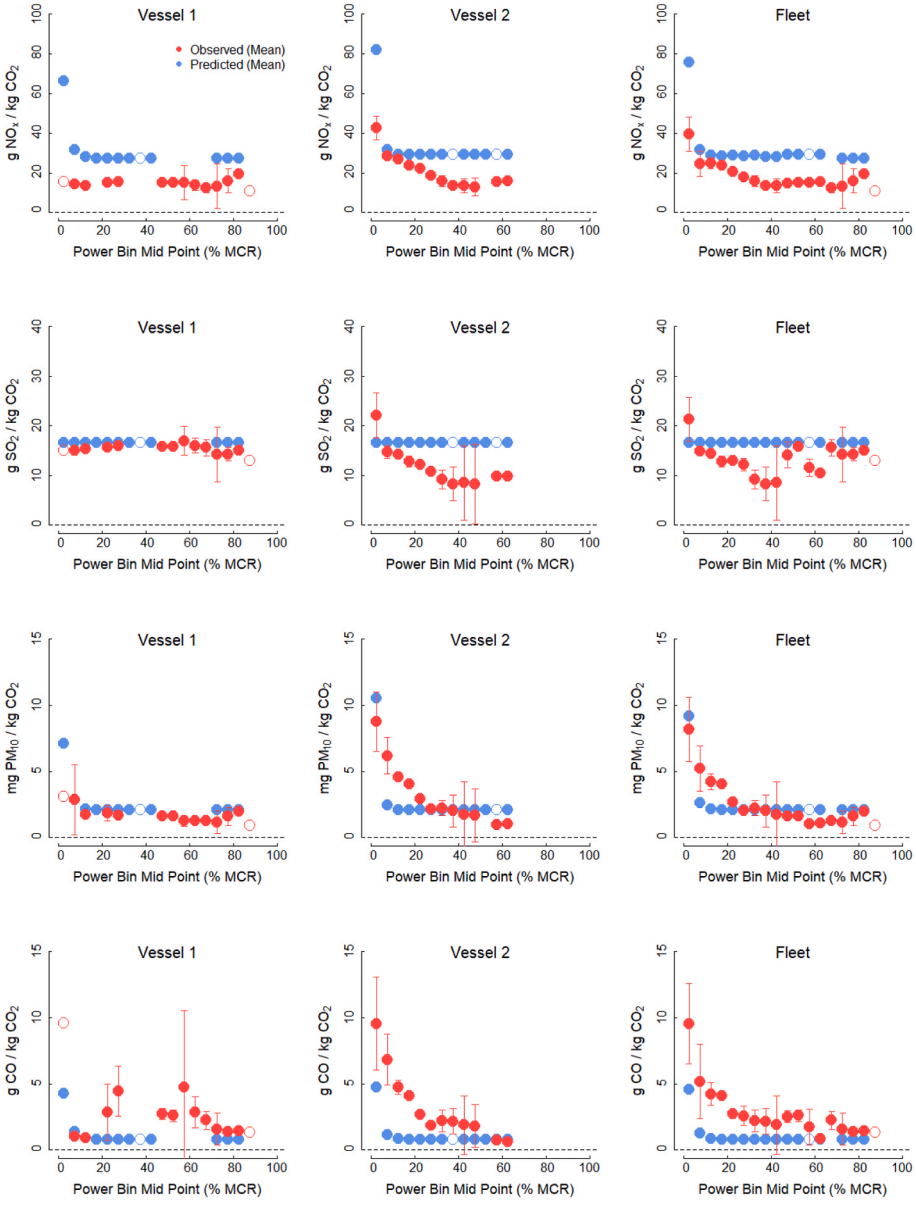

Fig. 5. Measured and predicted emission ratios for four air pollutants, two levels of aggregation and twenty power bins, including the 95% confidence intervals for measured emission factors and the range (min-max) for predicted emission factors. Open dots represent bins with only one value.

Table 4
Performance statistics for emission ratios by vessel.

Pollutant	Vessel	r	R^2	MAE (kg/min[a])	MPE	NRMSE
NO_x	Vessel 1	0.00	0.00	17.52	117%	347%
	Vessel 2	0.80	0.65	12.89	69%	54%
	Fleet	0.83	0.69	12.62	71%	55%
SO_2	Vessel 1	0.32	0.15	1.51	10%	96%
	Vessel 2	−0.05	0.01	5.77	53%	44%
	Fleet	−0.07	0.01	4.05	34%	36%
PM_{10}	Vessel 1	0.76	0.58	0.84	39%	78%
	Vessel 2	0.77	0.59	1.17	8%	20%
	Fleet	0.80	0.64	0.85	16%	16%
CO	Vessel 1	0.88	0.77	1.67	−39%	28%
	Vessel 2	0.79	0.62	2.14	−52%	31%
	Fleet	0.87	0.77	1.85	−59%	26%

[a] For PM_{10} the unit is g/min.

with flat emission ratios above 20% MCR and increasing ratios below 20% MCR. The measurements for Vessel 1 show a similar emission profile (with some expected variability), but without a clear upward or downward trend. For Vessel 2, the measured profile is different with a downward trend in emission ratios with increasing engine power for all pollutants, although the uncertainty for specific power bins can be large as shown by the extent of the confidence intervals of the mean.

The modelled emission ratios for Vessel 1 show good agreement for SO_2 and a reasonable agreement for PM_{10} and CO, with mean prediction errors within 10% and 40%, respectively. For NO_x, emission ratios used in the model overestimate observed ratios with a factor of about two. The modelled emission ratios for Vessel 2 show good agreement for PM_{10} and a moderate agreement for SO_2 and CO, with mean prediction errors within about 10% and 50%, respectively. For NO_x, emission ratios used in the model overestimate observed ratios with about 70%. At fleet level, model performance tends to present the average performance for the two vessels, resulting in good overall performance for SO_2 and PM_{10}, moderate performance for CO and poor performance for NO_x (bias: significant overestimation).

The SO_2/CO_2 ratio from on-board measurements observed for Vessel 2 presented in Fig. 5 varied significantly compared to that from Vessel 1. This ratio would be expected to be theoretically constant throughout engine load conditions. However, in the real world, the proportion of fuel sulphur and fuel carbon contributes to particular matter emissions, resulting in variability in their conversion rate to the gas phase. Therefore, while SO_2/CO_2 ratio may be constant during some on-board measurements it is not surprising that it may vary with others, depending on the ship operating conditions. The variation in SO_2/CO_2 ratio can also be found in previous studies (Bai et al., 2020; Yang et al., 2022).

3.4. Assessment of model performance (Method 2)

In this section emission model performance is assessed after normalising for engine power. Fig. 6 (next page) compares mean observed and predicted emission factors, expressed as (k)g/min, for all pollutants and twenty-one engine power bins, where power is expressed as % MCR (0–100% in 5% increments). The 95% confidence intervals are included for measured emission factors, as well as the range of predictions in each power bin, whenever data are available. Table 5 presents an overview of model performance statistics.

The prediction performance for CO_2, NO_x, SO_2 and PM_{10} is good for Vessel 1 with a high level of correlation and a mean prediction error within ±40%. In addition, predictions often fall within the 95% confidence intervals of the measured values suggesting that predictions are made within the uncertainty of the measurements. The results for CO suggest a significant underestimation with a mean prediction error of about −60%. For Vessel 2, performance for CO_2, NO_x, SO_2 and PM_{10} is also good with a high level of correlation and a mean prediction error within ±40%. For PM_{10} the mean prediction error is very good (±10%), but correlation is poor, which is caused by a flat relationship between power and observed PM emission factors. The results for CO again suggest a significant underestimation with a mean prediction error of about −60%. At fleet level (combining data for both vessels), *r* and R^2 prediction performance is generally reduced, but prediction errors can improve in some cases (CO_2, SO_2).

In conclusion, the observed emission factors follow the general direction of the modelled emission factors: an increase in emission rates with increasing engine power. In a few cases (Vessel 2, PM and CO), the observed emission factors are (more or less) constant, which reduces the level of agreement with emission factors used in the model. Prediction performance varies substantially with pollutant and vessel. Performance can be good with good correlation and small prediction errors (for instance CO_2 for Vessel 1 and 2) or poor with large discrepancies (for instance CO for Vessel 1 and 2). Nevertheless, the observed and modelled emission factors generally fall within a similar range of values.

3.5. Assessment of model performance (Method 3)

In this section emission model performance is assessed for the entire emission prediction process, namely AIS processing, prediction of fuel consumption and applying fuel-based emission factors. The goodness-of-fit plots are shown for all vessels and pollutants in Fig. 7 using the UTM method. Observed and predicted emission factors are compared for 1 km segments and the longer measurement period. In addition, the 1 km segment results for vessels 1 and 2 are combined (fleet) to assess overall prediction performance.

The information presented in Table 3 (Section 3.2) and Fig. 7 provide the following insights. For 1 km emission factors the correlation between predictions and observations is negative, which means that generally observations increase when predictions decrease, and vice versa. With a negative correlation coefficient, consideration of R^2 is not useful. It implies that predictions applied at 1 km grid level may generate issues when relative changes in ship emissions are modelled. However, this counter intuitive and unfavourable outcome regarding the direction of the predictions is the result of spatial and temporal inaccuracies in linking AIS data to the on-board measurements. It is unlikely to be an issue with the prediction algorithms, as was shown in the previous sections with reasonable to good agreement in terms of predicted and observed emission factors.

It was clear in Fig. 4 that the correspondence between recorded main engine power (kW) during the test program and predicted main engine power using AIS data in combination with the ship emissions model was reasonable for some measurement periods but poor for others, which shows that there is an issue with matching AIS data with on-board measurements in some periods.

It is noted that proper alignment of AIS and on-board test data was thoroughly investigated and checked during this study. Time stamps of the on-board testing program were verified by going back to the raw measurement data. However, matching of AIS and emission test data could not be improved for some measurement periods.

In the absence of other independent data sets, it is unclear if these discrepancies are caused by time stamp issues in on-board measurements or positional or other issues (e.g. shifts) in the AIS data. We suggest this is a further avenue for research as accurate input data are critical for global, regional and local ship emission inventories. We point out that accuracy issues with speed and positional AIS data, even after throrough verification and post-processing, is not beyond the realm of possibilities. For instance, refer to Emmens et al. (2021) who provide a detailed examination of the strengths and weaknesses of AIS data. They stated that the process of AIS data cleaning is 'rather difficult'.

In contrast to direction, the magnitude of the errors appears reasonable, particularly for NO_x and SO_2 where the MPE lies within approximately ±5% and ±15%, respectively. For PM_{10} and CO_2 the prediction error is higher and MPE lies within approximately ±30% and ±40%, respectively. The prediction error for CO is large, where

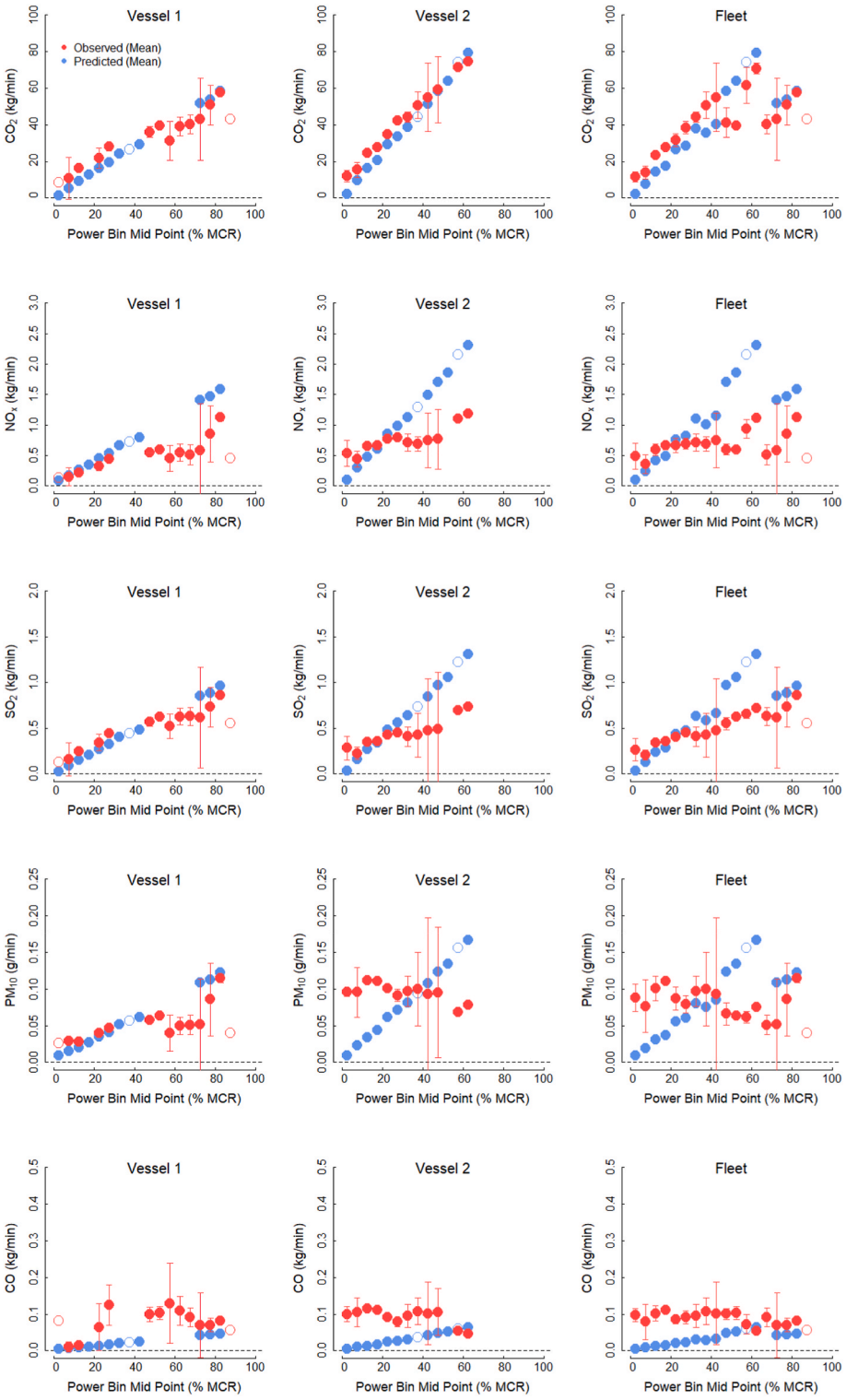

Fig. 6. Measured and predicted emission factors for five pollutants, two levels of aggregation and twenty power bins, including the 95% confidence intervals for measured emission factors and the range (min-max) for predicted emission factors. Open dots represent bins with only one value.

observations suggest a significant and consistent underestimation (bias) in predicted values. Whereas predicted CO emission factors vary between 0.003 and 0.15 kg/km, observed values are ranging from 0.04 to 2.26 kg/km, which is in line with issue with the emission factors discussed in Section 3.3 and 3.4. Fig. 5 shows that spatial aggregation improves model performance. This can be seen when the average emission factors for the three measurement periods are considered for vessel 1 and 2 (large black open dots). The positions of theses dots move closer to the 45° line, which presents a perfect fit between observations and predictions.

Table 6 presents the performance statistics for *aggregated* vessel movements. It includes the calculated overall model performance when the grand mean is compared for both observations and predictions. The result is shown in Table 6 (Vessel = Fleet), as well as the Fleet plots in

Table 5
Performance statistics for power normalised emission factors by vessel.

Pollutant	Vessel	r	R^2	MAE (kg/min[a])	MPE	NRMSE
CO_2	Vessel 1	0.99	0.97	5.66	−25%	13%
	Vessel 2	1.00	0.99	5.68	−20%	10%
	Fleet	0.88	0.77	10.07	−10%	19%
NO_x	Vessel 1	0.94	0.88	0.28	39%	41%
	Vessel 2	0.90	0.80	0.50	37%	84%
	Fleet	0.70	0.48	0.55	57%	90%
SO_2	Vessel 1	0.97	0.95	0.12	−18%	18%
	Vessel 2	0.95	0.90	0.26	29%	63%
	Fleet	0.88	0.78	0.23	22%	44%
PM_{10}	Vessel 1	0.88	0.77	0.02	−2%	28%
	Vessel 2	−0.74	0.55	0.05	−8%	136%
	Fleet	−0.44	0.20	0.05	14%	90%
CO	Vessel 1	0.32	0.10	0.04	−58%	47%
	Vessel 2	−0.72	0.51	0.07	−58%	104%
	Fleet	−0.53	0.28	0.06	−59%	108%

[a] For PM_{10} the unit is g/min.

Fig. 7 (solid black dot).

Spatial aggregation significantly improves model performance. The correlation coefficient becomes positive and can be strong in some cases (for instance NO_x Vessel 1). This is relevant for ship emission inventories as spatial aggregation will increase the robustness of the emission modelling results. It also confirms that the ship emissions model should be applied at the lower spatial and temporal resolution for which it is designed, as was discussed in Section 2.6.

The magnitude of prediction errors (MAE) is significantly reduced for all substances at fleet level when compared with 1 km segments (Table 3), except for CO with the same error.

3.6. The impact of current data on predicted emissions

Current information was available only for a portion of the on-board testing data. The results are included in the goodness-of-fit plots in the Supplementary Information (SM2). There is a negligible difference for Vessel 1, as was already discussed in Section 3.1. For Vessel 2, there are some differences between model predictions with and without local current information. The impact on model performance is summarised in Table 7.

Improved model performance through inclusion of local current information is indicated in bold font. Depending on the pollutant and performance statistic, prediction results may improve or may deteriorate. In terms of prediction errors (MAE, MPE, NRMSE) results improve when current information is included in the calculation for all substances, except PM_{10}. In terms of correlation I, performance deteriorates further with inclusion of current for all substances, except CO. In all cases, changes in model performance are marginal, which suggests the extra effort of accounting for local currents in ship emission inventories may not be cost-effective. However, we note that this would obviously depend on the actual location. The currents experienced by vessels in this study were not particularly strong (with a maximum of approximately 1 knots). In areas where vessels experience strong currents, it is expected that currents will have a significant impact on fuel consumption and emissions.

3.7. Further guidance for on-board emission testing on ships

The discrepancy between AIS data and on-board emissions testing for some measurement periods found in this paper highlights the need for internationally agreed guidance regarding on-board ship emission measurements. Based on the findings of this study the following recommendations are made:

- Measurement of date/time stamped location and ideally speed should be made and recorded simultaneously to emission measurements using GPS equipment, and time aligned with engine emission and engine parameters.
- GPS measurements should be made independently of the AIS equipment. A difficulty arises because the emission and engine measurements will be made in the ship engine room or adjacent to the exhaust stack, which will be isolated from satellite reception inside the ship structure. The GPS will need to be located above the ship superstructure and logged there or connected (probably by cable) to the emission and engine logging system.
- The sampling frequency should be at least as fast as the sampling frequency of the emission measurements or AIS (whichever is faster).
- A spatial resolution of at least 10 m should be used.

Given the common use of AIS data in ship emission inventories, it would be of interest to examine the level of agreement between AIS data and GPS data collected on-board in future studies.

4. Conclusions

This study has used on-board emission testing data for two ocean-going vessels to assess the performance of an Australian ship emissions model, and to assess the impact of local currents. Since the on-board testing program did not collect geographic location or vessel speed and course, ship movement information was independently obtained using post-processed and verified Automatic Identification System (AIS) data. Time-series (location, speed/course over ground) were created using different computation methods (spatial interpolation, imputation of spot speeds). In addition, local sea current data were used to compute corrected speeds (speed over water). The six different time-series of speed were then used as input to the ship emissions model to predict fuel use, emissions and main engine power. This information was combined with the on-board emission testing results to create a performance assessment database (1 min time resolution).

It was found that the choice of AIS post-processing method can have a significant effect on predicted vessel speeds up to a maximum of about 2 knots, but that, on average, differences are small in the order of 5%. The impact of local currents on main engine power was found to be negligible for one vessel, but potentially significant at specific points in time for the second vessel, varying between ±10% MCR. The correspondence between recorded and estimated main engine power (kW) was good for some measurement periods but poor for others, which suggests that there are potentially unresolved issues with matching AIS data with on-board emissions tetsing. In the absence of other independent data sets, it is unclear if these discrepancies are caused by time stamp issues in on-board measurements or positional issues (shifts) in the AIS data and further research is recommended. We also suggest the development of internationally agreed guidelines for on-board emissions testing and make some recommendations regarding the spatial-temporal aspects of emissions data collection.

It was found that AIS post-processing method did only marginally affect prediction performance and that none of the methods stood out as being the best approach. Similarly, only a marginal improvement was observed after inclusion of current impacts in emission modelling. This suggests the extra effort of accounting for local currents in ship emission inventories may not be cost-effective. However, the currents experienced by vessels in this study were not particularly strong. In areas where vessels experience strong currents, it is expected that currents will have a significant impact on fuel consumption and emissions.

Model performance was assessed for three different aspects, fuel-based emission factors (g/g CO_2), engine work-based emission factors (g/kWh) and distance-based emission factors (g/km). In terms of fleet level results:

1. Analysis of fuel-based emission factors suggest that predicted values for NO_x are biased high with a significant overestimation of about 70% on average. In contrast, predicted values for CO are biased low

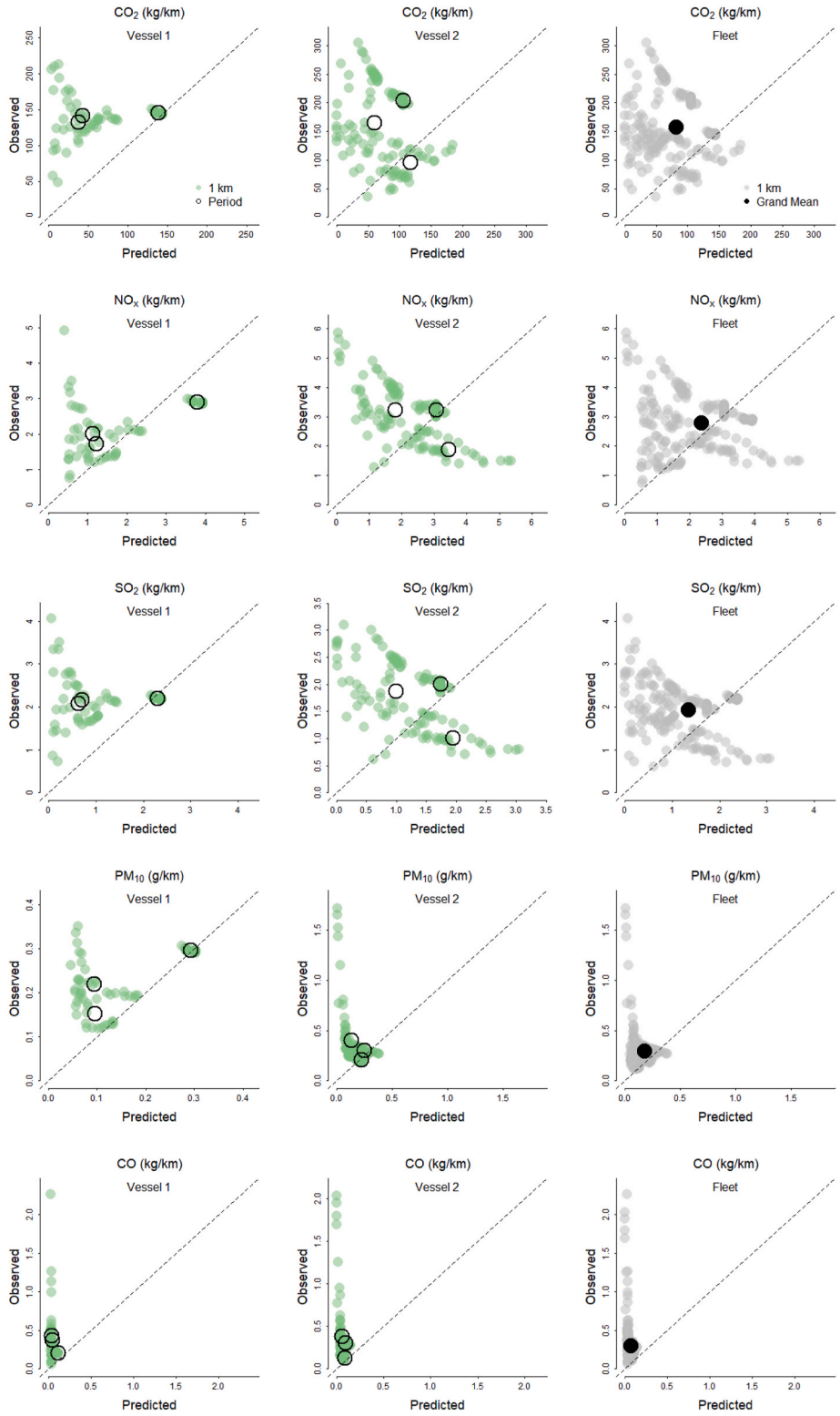

Fig. 7. Goodness-of-fit plots showing measured versus predicted emission factors for two vessels, combined (fleet), five pollutants and two levels of aggregation (UTM post-processing method).

with a significant underestimation of about 60% on average. The level of agreement between observed and predicted fuel-based emission factors is reasonable to good for PM_{10} and SO_2. The relationship with engine power is replicated well for one vessel but not the other one. However, we acknowledge the small sample size of this study and recommend on-board testing on more vessels and pooling emissions data from previous studies would be required to confirm the general shape of the relationship with engine power.

2. Analysis of work-based emission factors generally shows improved performance, which suggest that errors in fuel use estimation and fuel-based emission factors tend to offset each other. The observed emission factors follow the general direction of the modelled

Table 6
Performance statistics for aggregated vessel movements by vessel (UTM post-processing method).

Pollutant	Vessel	r	R^2	MAE (kg/km[a])	MPE	NRMSE
CO_2	Vessel 1	0.75	0.57	67.26	−49%	614%
	Vessel 2	−0.35	0.12	75.61	−30%	78%
	Fleet	–	–	64.34	**−44%**	–
NO_x	Vessel 1	0.97	0.93	0.76	−14%	67%
	Vessel 2	−0.68	0.46	1.05	11%	91%
	Fleet	–	–	0.10	**−4%**	–
SO_2	Vessel 1	0.70	0.48	1.01	−44%	1010%
	Vessel 2	−0.57	0.33	0.69	10%	76%
	Fleet	–	–	0.51	**−27%**	–
PM_{10}	Vessel 1	0.88	0.77	0.06	−32%	56%
	Vessel 2	−0.72	0.52	0.11	−27%	83%
	Fleet	–	–	0.08	**−32%**	–
CO	Vessel 1	−0.98	0.96	0.28	−76%	136%
	Vessel 2	−0.52	0.27	0.20	−64%	92%
	Fleet	–	–	0.24	**−77%**	–

[a] For PM_{10} the unit is g/km.

Table 7
Performance statistics for Vessel 2 excluding/including local current information (UTM post-processing method).

Pollutant	Vessel	r	R^2	MAE (kg/km[a])	MPE	NRMSE
CO_2	Excluded	**−0.50**	0.25	100.10	−49%	486%
	Included	−0.68	0.46	**90.34**	**−45%**	**466%**
NO_x	Excluded	**−0.23**	0.05	0.20	−5%	55%
	Included	−0.39	0.15	**0.15**	**2%**	**47%**
SO_2	Excluded	**−0.52**	0.27	0.27	−13%	86%
	Included	−0.66	0.44	**0.17**	**−7%**	**58%**
PM_{10}	Excluded	**0.02**	0.00	0.02	6%	35%
	Included	−0.29	0.08	0.03	15%	58%
CO	Excluded	−0.37	0.13	0.05	−36%	78%
	Included	**−0.13**	0.02	**0.04**	**−31%**	**72%**

[a] For PM_{10} the unit is g/km.

emission factors: an increase in emission rates with increasing engine power, with a few exceptions, showing natural variability between ships. Prediction performance for CO_2 is good and within ±10%. Predicted values for NO_x are biased high with a significant overestimation of about 60% on average. In contrast, predicted values for CO are biased low with a significant underestimation of about 60% on average. The level of agreement between observed and predicted fuel-based emission factors is good for PM_{10} and SO_2 and within approximately ±15% and ±20%, respectively. The observed and modelled emission factors generally fall within a similar range of values.

3. Analysis of distance-based emission factors generally showed the largest discrepancies between predicted and observed values. The results suggest that the main cause is related to spatial and temporal differences between on-board testing and AIS data. These differences can lead to artificial improvements in model performance. For instance, NO_x predictions are very good with prediction errors within approximately ±5%. This is despite the significant bias observed in fuel-based and work-based emission factors. The assessment of model performance for distance-based emission factors therefore has limited meaning in this study. This can only change once better matching of AIS and emissions data are achieved, which we have been unable to do in this specific study despite substantial efforts. Given the importance of AIS data in emissions modelling, it is recommended that the spatial and temporal accuracy of AIS data is investigated and confirmed in future studies. Moreover, the discrepancies found in this study between model predictions and on-board measurements highlight some limitations in application of generic fleet-based models.

CRediT authorship contribution statement

Robin Smit: Conceptualization, Methodology, Software, Data curation, Writing – original draft, preparation, Visualization, Investigation, Supervision, Writing – review & editing. **Thuy Chu-Van:** Methodology, Data curation, Writing – original draft, preparation, Visualization, Investigation. **Kabir Suara:** Methodology, Software, Data curation, Writing – original draft, preparation, Investigation. **Richard J. Brown:** Conceptualization, Methodology, Supervision, Writing – review & editing.

Declaration of competing interest

The authors declare that they have no known competing financial interests or personal relationships that could have appeared to influence the work reported in this paper.

Data availability

Data will be made available on request.

Acknowledgements

The authors gratefully acknowledge the Port of Brisbane Corporation for their ongoing support of the project, Maritime Safety Queensland and stevedore operators (AAT, Patricks and DP World). The authors would like to acknowledge the outstanding support received from all employees and crew of CSL Group Inc. A special thanks to Ms Rhiannah Carver and Mr Jovito Barrozo from CSL Australia for their assistance in coordinating this project. In addition, the materials and data in this publication have been obtained through the support of the International Association of Maritime Universities (IAMU) and the Nippon Foundation in Japan.

Appendix A. Supplementary data

Supplementary data to this article can be found online at https://doi.org/10.1016/j.aeaoa.2022.100192.

References

Bai, C., Li, Y., Liu, B., Zhang, Z., Wu, P., 2020. Gaseous emissions from a seagoing ship under different operating conditions in the coastal region of China. Atmosphere 11, 305.

Baird, M.E., Green, R., Lowe, R., Mongin, M., Bougeot, E., 2020. Optimising cool-water injections to reduce thermal stress on coral reefs of the Great Barrier Reef. PLoS One 15 (10), e0239978.

CARB, 2022. 2021 California Ocean-Going Vessels Emission Inventory. California Air Resources Board (CARB), 3 March 2022. https://ww2.arb.ca.gov/our-work/programs/mobile-source-emissions-inventory/road-documentation/msei-documentation-road.

Chu-Van, T., Ristovski, Z., Pourkhesalian, A.M., Rainey, T., Garaniya, V., Abbassi, R., Jahangiri, S., Enshaei, H., Kam, U.S., Kimball, R., Yang, L., Zare, A., Bartlett, H., Brown, R.J., 2018. On-board measurements of particle and gaseous emissions from a large cargo vessel at different operating conditions. Environ. Pollut. 237, 832–841.

Chu-Van, T., Ristovski, Z., Pourkhesalian, A.M., Rainey, T., Garaniya, V., Abbassi, R., Kimball, R., Luong Cong, N., Jahangiri, S., Brown, R.J., 2019. A comparison of particulate matter and gaseous emission factors from two large cargo vessels during manoeuvring conditions. Energy Rep. 5, 1390–1398.

Corbett, J.J., Winebrake, J.J., Green, E.H., Kasibhatla, P., Eyring, V., Lauer, A., 2007. Mortality from ship emissions: a global assessment. Environ. Sci. Technol. 41 (24), 8512–8518.

DES, 2019. *Simulation And Assessment Of Shipping Fuel Consumption And Emissions And Their Potential Local Air Quality Impacts - 15 Queensland Strategic Ports*, Prepared by: Robin Smit, Phil Kingston, Alice Militon, Miguel Alvarado. Queensland Government, Department of Science and Environment, Brisbane, Australia. https://nla.gov.au/nla.obj-1371565938/view.

eReef, 2021. eReefs GBR Model Data/eReefs GBR4 hydrodynamic_v2. retrieved from. https://dapds00.nci.org.au/thredds/dodsC/fx3/model_data/gbr4_2.0.ncml.

EEA, 2013. The Impact of International Shipping on European Air Quality and Climate Forcing. European Environment Agency. Technical report No. 4/2013.

EMEP/EEA, 2016. International navigation, national navigation, national fishing, EMEP/EEA emission inventory Guidebook 2013, European monitoring and evaluation

programme (EMEP), European environment agency (EEA), by trozzi, C., de lauretis, R. https://www.researchgate.net/publication/273098351_EMEPEEA_air_pollutant_emission_inventory_guidebook_-_2013_1A3di_1A3dii_1A4ciii_International_navigation_national_navigation_national_fishing.

EMEP/EEA, 2021. international navigation, national navigation, national fishing, EMEP/EEA emission inventory Guidebook 2019 - update dec 2021, European monitoring and evaluation programme (EMEP), European environment agency (EEA), by de lauretis, R., ntziachristos, L., trozzi, C. https://www.eea.europa.eu/publications/emep-eea-guidebook-2019/part-b-sectoral-guidance-chapters/1-energy/1-a-combustion/1-a-3-d-navigation/view.

Emmens, T., Amrit, C., Abdi, A., Ghosh, M., 2021. The promises and perils of Automatic Identification System data. Expert Syst. Appl. 178, 114975 https://doi.org/10.1016/j.eswa.2021.114975.

Ghosh, A., Suara, K., Soomere, T., Brown, R.J., 2022. Using Lagrangian coherent structures to investigate upwelling and physical process in the Gladstone coastal region. J. Mar. Syst. 230, 103731.

Grigoriadis, A., Mamarikas, S., Ioannidis, I., Majamäki, E., Jalkanen, J.-P., Ntziachristos, L., 2021. Development of exhaust emission factors for vessels: a review and meta-analysis of available data. Atmos. Environ. X 12, 100142. https://doi.org/10.1016/j.aeaoa.2021.100142.

Herzfeld, M., Andrewartha, J., Baird, M., Brinkman, R., Furnas, M., Gillibrand, P., Hemer, M., Joehnk, K., Jones, E., McKinnon, D., Margvelashvili, N., Mongin, M., Oke, P., Rizwi, F., Robson, B., Seaton, S., Skerratt, J., Tonin, H., Wild-Allen, K., 2016. eReefs Marine Modelling: Final Report, Jan. 2016. CSIRO, Hobart, pp. 1–497.

Khan, M.Y., Ranganathan, S., Agrawal, H., Welch, W.A., Laroo, C., Miller, J.W., Cocker, D.R., 2013. Measuring in-use ship emissions with international and U.S. federal methods. J. Air Waste Manag. Assoc. 63, 284–291.

Liu, H., Fu, M., Jin, X., Shang, Y., Schindell, D., Faluvegi, G., Schindell, C., He, K., 2016. Health and climate impacts of ocean-going vessels in East Asia. Nat. Clim. Change 1–5.

Skerratt, J.H., Mongin, M., Baird, M.E., Wild-Allen, K.A., Robson, B.J., Schaffelke, B., Steven, A.D.L., 2019. Simulated nutrient and plankton dynamics in the Great barrier Reef (2011-2016). J. Mar. Syst. 192, 51–74.

Smit, R., Awadallah, M., Bagheri, S., Surawski, N.C., 2022. Real-world Emission Factors for SUVs Using On-Board Emission Testing and Geo-Computation, vol. 103286. Transp. Res.-D, pp. 1–21. https://doi.org/10.1016/j.trd.2022.103286.

Suara, K., Khanarmuei, M., Ghosh, A., Yu, Y., Zhang, H., Soomere, T., Brown, R.J., 2020. Material and debris transport patterns in Moreton Bay, Australia: the influence of Lagrangian coherent structures. Sci. Total Environ. 721, 137715.

US EPA, 2022. Ports Emissions Inventory Guidance: Methodologies for Estimating Port-Related and Goods Movement Mobile Source Emissions. U.S. Environmental Protection Agency (US EPA), Transportation and Climate Division, Office of Transportation and Air Quality. EPA-420-B-22-011, April 2022. https://www.epa.gov/state-and-local-transportation/port-emissions-inventory-guidance.

Yang, L., Zhang, Q., Zhang, Y., Lv, Z., Wu, L., Mao, H., 2022. Real-world emission characteristics of an ocean-going vessel through long sailing measurement. Sci. Total Environ. 810, 152276.